A New Approach to Superdirective Arrays

A. Z. ROBINSON

Methods and Systems Branch
Underwater Sound Reference Division

January 5, 1971

Contents

Illustrations

Tables

Abstract

The concept of defined nulls in the directional response of arrays and the introduction of electrical delays to achieve the desired placement of the nulls provide a new approach to acoustical superdirective arrays. The shading that results is a variant of binomial shading in that the number of times a given element contributes to the array output is determined by the appropriate binomial coefficient, but the signal from the element undergoes a possibly different electrical delay each time the element contributes. For an end-fire condition, the maximum array gain (assuming isotropic noise) is equal to the square of the number of elements in the array. The methods used yield results for three- and five-element broadside arrays that are equivalent to those obtained earlier by R. L. Pritchard. The type of array described responds to a higher order gradient of the pressure field rather than to the pressure field itself. A digital method for implementation of such an array is presented.

Problem Status

This is an interim report.

Problem Authorization

A NEW APPROACH TO SUPERDIRECTIVE ARRAYS

Introduction

Arrays of essentially point receiving elements are used in a large number of Navy underwater acoustic systems to achieve directional response. As a general rule, the outputs of these elements are steered by electrical delays so that all steered outputs resulting from signals arriving from a preferred direction in space are in time coincidence. The summation of these steered outputs then gives a directional response that consists of a main lobe in the desired direction and secondary or side lobes in other directions.

These side lobes can be quite troublesome and can lead to ambiguous interpretations of the array output. Dolph [1] developed a method of shading for linear arrays to control the level of this undesired side-lobe response. His method consists of adjusting the amplitude weighting of each element so as to force the response function into the form of a Tschebyscheff polynomial of appropriate order with an appropriate end point. For such shading, the levels of all side lobes are the same. The magnitude of the side-lobe response relative to the main-lobe response is controlled by the choice of the end point for the Tschebyscheff polynomial. The design procedure, then, is to select an acceptable side-lobe response and use this to compute the magnitude of the shading factors. The price paid for such side-lobe suppression is broadening of the main lobe.

The original method as proposed by Dolph was valid only for element spacings of one-half wavelength or greater. Riblet [2] showed that the application of Dolph's method to very small element spacings (less than one-half wavelength) resulted in rapid phase reversals in antenna current distributions, which is characteristic of "super gain" antennas. The work of both Dolph and Riblet was applied principally to antenna theory.

Pritchard [3,4,5,6] has studied acoustical arrays from the standpoint of optimized response characteristics. He has applied the methods of Dolph to acoustical arrays and has shown that narrow-beam directional response can be achieved with relatively short arrays in which the element spacing is much less than one-half wavelength. The element shading factors, in this case, alternate in sign, which corresponds to the "rapid phase reversal in distribution current" reported by Riblet. Pritchard notes this similarity and refers to acoustical arrays with small element spacing and alternating signs in the shading factors as "super gain" or "superdirective" arrays. Pritchard, in general, limited his studies to

1

arrays for which the main lobe is normal to the axis of the array and to excitation by discrete frequencies or very narrow-band sources.

Broadband excitation of these superdirective arrays and main-lobe response along the axis of the array (end fire) are considered in this report. A method for achieving the desired response by using electrical delays and a variant of binomial shading will be developed. With this method, optimized responses (based upon maximization of the directivity index) will be developed for both broadside and end-fire arrays and will be related to specified nulls in the directional response. Results obtained for broadside arrays having maximum directivity indices will be compared with the earlier work of Pritchard.

The sensitivity problem associated with superdirective arrays will be examined and compromises for solving this problem will be suggested. The report will show that the response of such arrays is related more to higher order field gradients than to the field itself, where the order of the most important gradient depends upon the number of elements involved. The practical application of superdirective arrays to Navy problems and a digital method for achieving the desired combination of elements will be presented.

Some Basic Mathematical Relationships

Before proceeding further, it is necessary to develop some basic mathematical relationships. Let

$$g(t) = f(t) - f(t - b_1).$$ (1)

Then

$$\text{Lim}_{b_1 \to 0} [g(t)] = b_1 \frac{\partial f(t)}{\partial t}.$$ (2)

Taking the Fourier transform of $g(t)$ gives

$$F_g(f) = \int_{-\infty}^{\infty} g(t) \, e^{-j\omega t} dt = \int_{-\infty}^{\infty} [f(t) - f(t - b_1)] \, e^{-j\omega t} dt$$

$$= F(f) [1 - e^{-j\omega b_1}],$$ (3)

where $j = \sqrt{-1}$, $\omega = 2\pi f$, f is frequency, and $F(f)$ is the Fourier transform of $f(t)$.

Next, let

$$h(t) = g(t) - g(t - b_2).$$ (4)

2

Then,

$$\mathop{\rm Lim}_{\substack{b_1 \to 0 \\ b_2 \to 0}} \left[h(t) \right] = b_2 \frac{\partial}{\partial t} \left\{ \mathop{\rm Lim}_{b_1 \to 0} \left[g(t) \right] \right\}$$

$$= b_1 b_2 \frac{\partial^2 f(t)}{\partial t^2}.$$

(5)

Substituting Eq. (1) into Eq. (4) gives

$$h(t) = f(t) - f(t - b_1) - f(t - b_2) + f(t - b_1 - b_2).$$

(6)

Taking the Fourier transform of $h(t)$ gives

$$F_h(f) = F_g(f) \left[1 - e^{-j\omega b_2} \right]$$

$$= F(f) \left[1 - e^{-j\omega b_1} \right] \left[1 - e^{-j\omega b_2} \right].$$

(7)

Next, let

$$k(t) = h(t) - h(t - b_3).$$

(8)

Then,

$$\mathop{\rm Lim}_{\substack{b_1 \to 0 \\ b_2 \to 0 \\ b_3 \to 0}} \left[k(t) \right] = b_1 b_2 b_3 \frac{\partial^3 f(t)}{\partial t^3}.$$

(9)

Substituting Eq. (6) into Eq. (8) gives

$$k(t) = f(t) - f(t - b_1) - f(t - b_2) - f(t - b_3) + f(t - b_1 - b_2)$$

$$+ f(t - b_1 - b_3) + f(t - b_2 - b_3)$$

$$- f(t - b_1 - b_2 - b_3).$$

(10)

The Fourier transform of $k(t)$ is given by

$$F_k(f) = F_h(f) \left[1 - e^{-j\omega b_3} \right]$$

$$= F(f) \prod_{i=1}^{3} (1 - e^{-j\omega b_i}).$$

(11)

If this method of successive differences is continued for n-fold differences, then

3

$$m(t) = f(t) - \sum_i^n f(t-b_i) + \sum_{i,j}^n f(t-b_i-b_j)$$

$$- \sum_{i,j,k}^n f(t-b_i-b_j-b_k) + \cdots (-1)^n f(t-b_1-b_2-\cdots-b_n),$$ (12)

where

$\sum_i^n$ indicates summation over all combinations of b taken one at a time

$\sum_{i,j}^n$ indicates summation over all combinations of b taken two at a time

$\sum_{i,j,k}^n$ indicates summation over all combinations of b taken three at a time

Also,

$$\lim_{\substack{b_1 \to 0 \\ \vdots \\ b_n \to 0}} [m(t)] = b_1 b_2 \cdots b_n \frac{\partial^n f(t)}{\partial t^n}.$$ (13)

The Fourier transform of m(t) is given by

$$F_m(f) = F(f) \prod_{i=1}^n (1 - e^{-j\omega b_i}).$$ (14)

The power spectral density of m(t) is given by

$$P_m(f) = F_m(f) F_m{}^*(f),$$ (15)

where $F_m{}^*(f)$ is the complex conjugate of $F_m(f)$. Then

$$P_m(f) = F(f)F^*(f) \prod_{i=1}^n (1 - e^{-j\omega b_i})(1 - e^{j\omega b_i})$$ (16)

$$= (4)^n P(f) \prod_{i=1}^n \sin^2(\omega b_1/2)$$

Array Configuration

Consider the five-element array shown in Fig. 1. The array is assumed to be in a plane-wave field where the normal to the wavefront is at an angle θ to the axis of the array. The acoustic pressure at the zero-th element (top of figure) is assumed to be p(t). The pressure at the ℓ-th element is then $p(t - \dfrac{\ell d}{c} \cos \theta)$, where d is the element spacing and c is the velocity of the wavefront. The spacing d is assumed to be less than one-half wavelength at the highest frequency to be considered, and $\tau_0 = d/c$ is the maximum acoustic delay between adjacent elements. The elements themselves are assumed to be point elements with identical omnidirectional sensitivities S. The electrical output of the ℓ-th element, then, is given by

$$f_\ell(t) = Sp(t - \ell\tau_0 \cos \theta). \tag{17}$$

Fig. 1. Five-element superdirective array.

The polarities of the electrical outputs of the odd-numbered elements of the array are reversed prior to any subsequent electrical delay. With the electrical delays shown in Fig. 1, the array output takes the form of Eq. (12) for n = 4, where

$$b_i = \tau_i + \tau_0 \cos \theta. \tag{18}$$

From Eq. (16), the power spectral density of the array output is given by

$$P_m(f) = (4)^4 P(f) \prod_{i=1}^{4} \sin^2[(\omega\tau_0/2)(\alpha_i + \cos\theta)], \tag{19}$$

where $\alpha_i = \tau_i/\tau_0$. Expressed in terms of element sensitivity and the power spectral density of p(t), this becomes

$$P_m(f) = (4)^4 S^2 P_p(f) \prod_{i=1}^{4} \sin^2[(\omega\tau_0/2)(\alpha_i + \cos\theta)], \tag{20}$$

where $P_p(f)$ is the power spectral density of p(t).

Assuming that $|\alpha_i| \le 1$, the directional response can be characterized by nulls in the directional response defined by

$$\theta_i = \cos^{-1}(-\alpha_i). \tag{21}$$

If τ_0 is allowed to approach zero and $|\tau_i| \le \tau_0$, then from Eq. (13) and Eq. (18)

$$m(t) = \left\{ \prod_{i=1}^{4} (\tau_i + \tau_0 \cos\theta) \right\} \frac{\partial^4 f(t)}{\partial t^4}. \tag{22}$$

Expressed in terms of the pressure field and the element sensitivity, this becomes

$$m(t) = S\left\{ \prod_{i=1}^{4} (\tau_i + \tau_0 \cos\theta) \right\} \frac{\partial^4 p(t)}{\partial t^4}. \tag{23}$$

Although the array of Fig. 1 is a five-element array, it is intended to illustrate the more general case of (n + 1) elements as well. For the array of (n + 1) elements, the electrical polarities of the odd-numbered elements are reversed prior to electrical delay. The ℓ-th element branches into $n!/\ell!(n - \ell)!$ lines, each with a delay that corresponds to the $n\tau_i$ taken ℓ at a time. Equations describing the response of the (n + 1)-element arrays are:

$$P_m(f) = (4)^n S^2 P_p(f) \prod_{i=1}^{n} \sin^2[(\omega\tau_0/2)(\alpha_i + \cos\theta)]; \tag{24}$$

and for $|\tau_i + \tau_0 \cos\theta| \ll 1$,

$$m(t) = S\left\{ \prod_{i=1}^{n} (\tau_i + \tau_0 \cos\theta) \right\} \frac{\partial^n p(t)}{\partial t^n}. \tag{25}$$

6

Maximum Directivity Index for End-Fire Superdirective Arrays

Consider an array of $(n + 1)$ elements analogous to the array of Fig. 1. The power spectral density of the output of this $(n + 1)$-element array is given by Eq. (24). If $\left|(\omega\tau_0/2)(\alpha_i + \cos\theta)\right| \ll 1$, Eq. (24) becomes

$$P_m(f) = (\omega\tau_0)^{2n}S^2P_p(f) \prod_{i=1}^{n}(\alpha_i + \cos\theta)^2 \tag{26a}$$

$$= K(a_1 + a_2\cos\theta + \cdots + a_n\cos^{n-1}\theta + \cos^n\theta)^2, \tag{26b}$$

where $K = (\omega\tau_0)^2S^2P_p(f)$ and the roots of the polynomial in $\cos\theta$ are $-\alpha_i$. The directivity index of this array for an end-fire condition $(\theta = 0°)$ is given by

$$\text{D.I.} = 10\log_{10} D, \tag{27}$$

where

$$D = \frac{4\pi\, F(\theta = 0)}{\displaystyle\int_0^\pi 2\pi\sin\theta\, F(\theta)\, d\theta}, \tag{28}$$

and

$$F(\theta) = (a_1 + a_2\cos\theta + \cdots + a_n\cos^{n-1}\theta + \cos^n\theta)^2. \tag{29}$$

Now,

$$\int_0^\pi \cos^i\theta\,\sin\theta\, d\theta = 2/(i + 1), \quad i \text{ even};$$

$$= 0 \quad\quad , \quad i \text{ odd}. \tag{30}$$

Therefore, for $n = 3$ (four elements), D_3 becomes

$$D_3 = \frac{(a_1 + a_2 + a_3 + 1)^2}{a_1^2 + (1/3)(a_2^2 + 2a_1a_3) + (1/5)(a_3^2 + 2a_2) + (1/7)}, \tag{31}$$

which can be maximized by taking its partial derivatives with respect to a_1, a_2, and a_3, setting these derivatives equal to zero, solving the resulting set of equations, and substituting back into Eq. (31). Values so derived for a_1, a_2, and a_3 are

$$a_1 = -3/35; \quad a_2 = -3/7; \quad a_3 = 3/7. \tag{32}$$

On substituting Eq. (32) back into Eq. (31), a maximum value for D_3 is obtained. This maximum is 16--the square of the number of elements involved.

7

This maximization process has been repeated for arrays with two through seven elements to determine the maximum directivity indices for the end-fire mode. In all cases, the maximum array gain D was the square of the number of elements in the array. In all cases considered, all of the roots of the derived polynomials in cos θ were real with an absolute value less than unity. This allows the directivity function to be expressed in terms of nulls in the directional response. A tabulation of the derived a_i for maximum gain is shown in Table I. The corresponding α_i and the associated nulls in the directional response are tabulated in Table II. Polar plots of the directional responses of these arrays are shown in Figs. 2-7.

Table I. Values of coefficients for maximum directivity index (end fire). $F(\theta) = [\cos^n\theta + \sum_{i=1}^{m} a_i \cos^{i-1}\theta]^2$. Number of elements is $n + 1$.

Number of elements	a_1	a_2	a_3	a_4	a_5	a_6
2	$+\dfrac{1}{3}$					
3	$-\dfrac{1\cdot3}{3\cdot5}$	$+\dfrac{2}{5}$				
4	$-\dfrac{1\cdot3}{5\cdot7}$	$-\dfrac{3}{7}$	$+\dfrac{3}{7}$			
5	$+\dfrac{1\cdot3\cdot5}{5\cdot7\cdot9}$	$-\dfrac{4}{21}$	$-\dfrac{2}{3}$	$+\dfrac{4}{9}$		
6	$+\dfrac{1\cdot3\cdot5}{7\cdot9\cdot11}$	$+\dfrac{5}{33}$	$-\dfrac{10}{33}$	$-\dfrac{10}{11}$	$+\dfrac{5}{11}$	
7	$-\dfrac{1\cdot3\cdot5\cdot7}{7\cdot9\cdot11\cdot13}$	$+\dfrac{10}{11\cdot13}$	$+\dfrac{45}{11\cdot13}$	$-\dfrac{60}{11\cdot13}$	$-\dfrac{15}{13}$	$+\dfrac{6}{13}$

Directional responses were generated in preceding paragraphs by assuming that the element spacings approach zero. The resulting array sensitivity for $\theta = 0$ in terms of element sensitivity can be computed from Eq. (26b); it is

$$S_m^{\,2} = (\omega\tau_0)^{2n}(a_1 + a_2 + \cdots + a_n + 1)s^2. \tag{33}$$

Since $\omega\tau_0 = 2\pi d/\lambda$ was allowed to approach zero, the corresponding array sensitivity also will approach zero. This is perhaps the biggest disadvantage of superdirective arrays. The sensitivity will be greatly

8

Table II. Description of nulls for superdirective end-fire arrays with maximum directivity index.

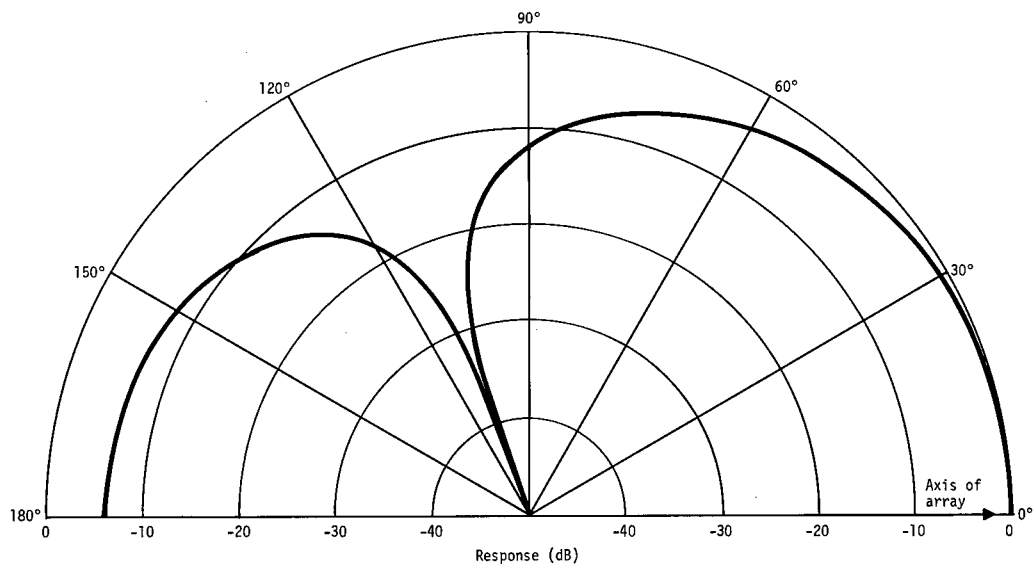| Number of elements	α_1	θ_1	α_2	θ_2	α_3	θ_3	α_4	θ_4	α_5	θ_5	α_6	θ_6
2	+0.33333	109.5°										
3	-0.28990	73.1°	+0.68990	136.4°								
4	-0.57532	54.9°	+0.18107	100.4°	+0.82282	145.4°						
5	-0.72048	43.9°	-0.16718	80.4°	+0.44631	116.5°	+0.88579	152.3°				
6	-0.80293	36.6°	-0.39093	67.0°	+0.12405	97.1°	+0.60397	128.2°	+0.92038	157.0°		
7	-0.85389	31.4°	-0.53847	57.4°	-0.11734	83.3°	+0.32603	109.0°	+0.70384	134.7°	+0.94137	160.3°

Fig. 2. Directional response of two-element superdirective array; maximum directivity index, end fire; three-dimensional response is the figure of revolution about the axis of the array; D.I. = 6 dB.
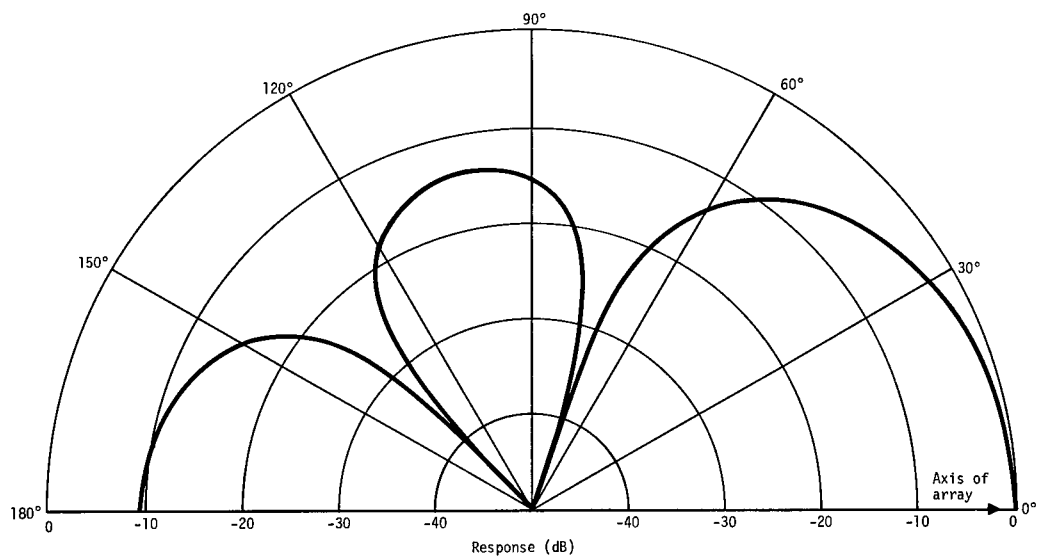

Fig. 3. Directional response of three-element superdirective array; maximum directivity index, end fire; three-dimensional response is the figure of revolution about the axis of the array; D.I. = 9.54 dB.
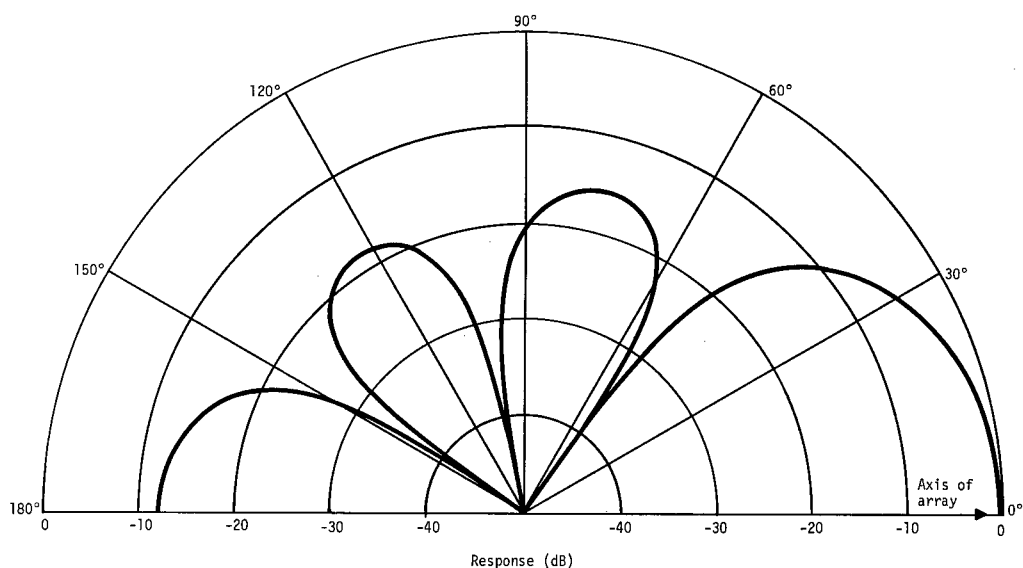
10

Fig. 4. Directional response of four-element superdirective array; maximum directivity index, end fire; three-dimensional response is the figure of revolution about the axis of the array; D.I. = 12.0 dB.
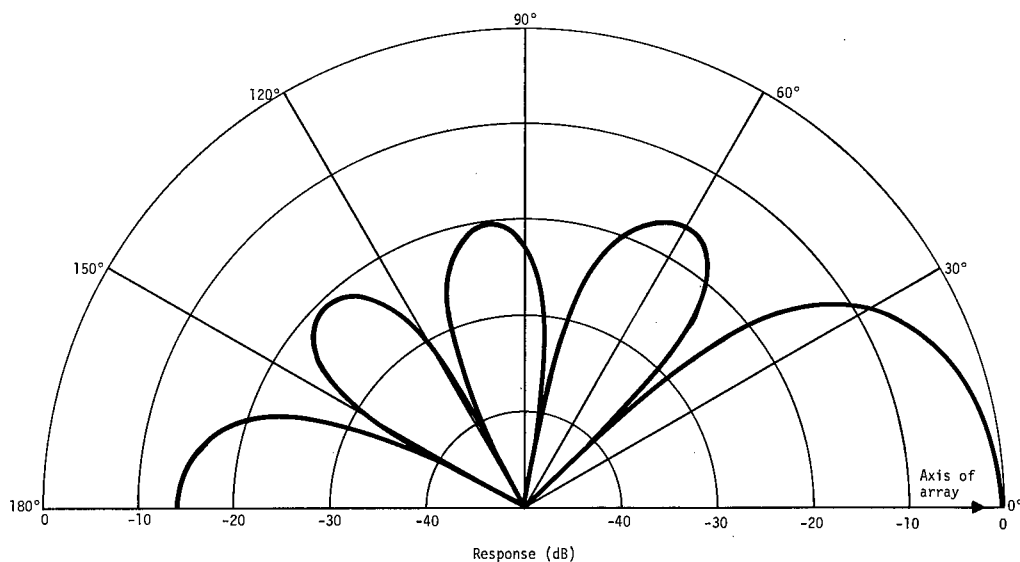

Fig. 5. Directional response of five-element superdirective array; maximum directivity index, end fire; three-dimensional response is the figure of revolution about the axis of the array; D.I. = 14.0 dB.
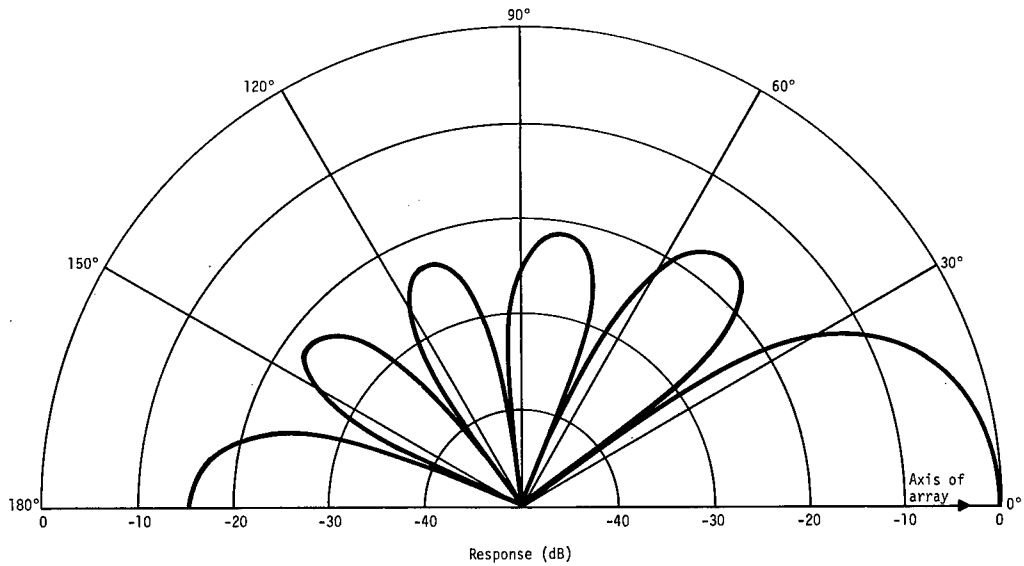
11

Fig. 6. Directional response of six-element superdirective
array; maximum directivity index, end fire; three-dimensional
response is the figure of revolution about the axis of the
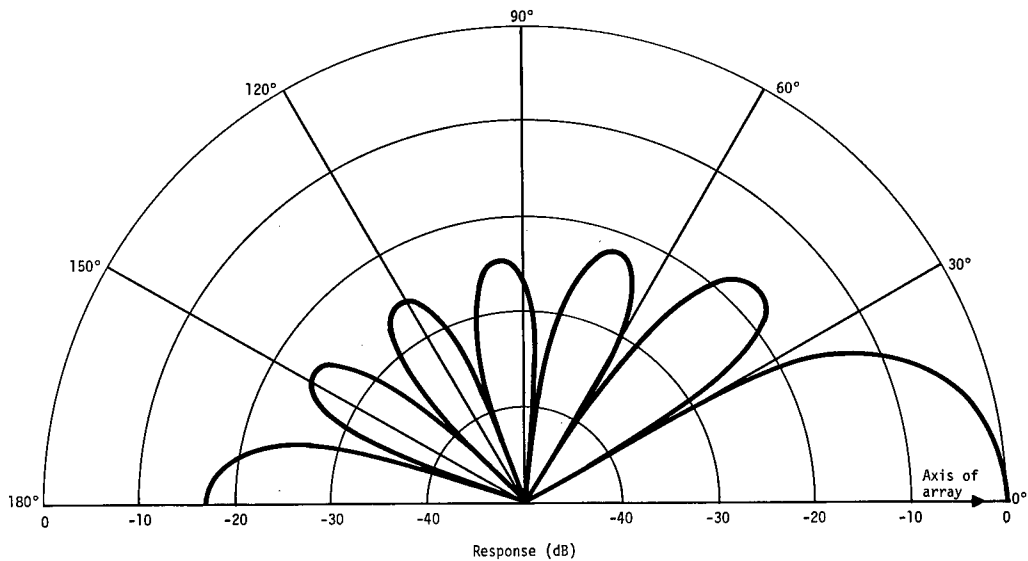array; D.I. = 15.56 dB.

Fig. 7. Directional response of seven-element superdirective
array; maximum directivity index, end fire; three-dimensional
response is the figure of revolution about the axis of the
array; D.I. = 16.9 dB.

12

improved, if the array spacing does not approach zero. On the other hand, the approximation of $P_m(f)$ given in Eq. (26a) can not be used in the calculation of the directivity indices. Instead,

$$F(\theta) = \prod_{i=1}^{n} \sin^2[(\omega\tau_0/2)(\alpha_i + \cos\theta)] \tag{34}$$

must be used. This $F(\theta)$ comes directly from Eq. (24). Directivity indices for various values of element spacing in a 6-element array, computed by using this value of $F(\theta)$ and the values of α_i derived from very small spacing, are plotted in Fig. 8. Note that even for an element spacing as large as $d = \lambda/\pi$, the directivity index has dropped only from 15.6 dB to about 13 dB. The sensitivity of the array for $\theta = 0$ and $d = \lambda/\pi$ now is given by

$$S_m^2 = (4)^5 S^2 \prod_{i=1}^{5} \sin^2(\alpha_i + 1),$$
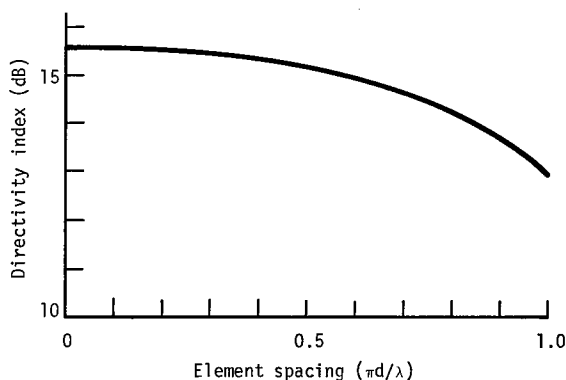
$$= 9.21\ S^2, \tag{35}$$

$$S_m = 3.04\ S.$$

Fig. 8. Directivity index of six-element superdirective array (end fire) as a function of element spacing.

To illustrate the effect of increased spacing on the directional response of superdirective arrays, the directional response shown in Fig. 6 (6-element array) is replotted on a different scale in Fig. 9 along with the directional response for an element spacing $d = \lambda/\pi$. The result of increasing the spacing is a slight broadening of the main lobe, and an increase in the side-lobe levels; however, side lobes still are more than 11 dB below the main lobe.

Maximum Directivity Index for Broadside Superdirective Arrays

It is interesting to compare the results obtained by using the methods of the preceeding section with Pritchard's results [6]. Pritchard considered only excitation by a single frequency and a primary
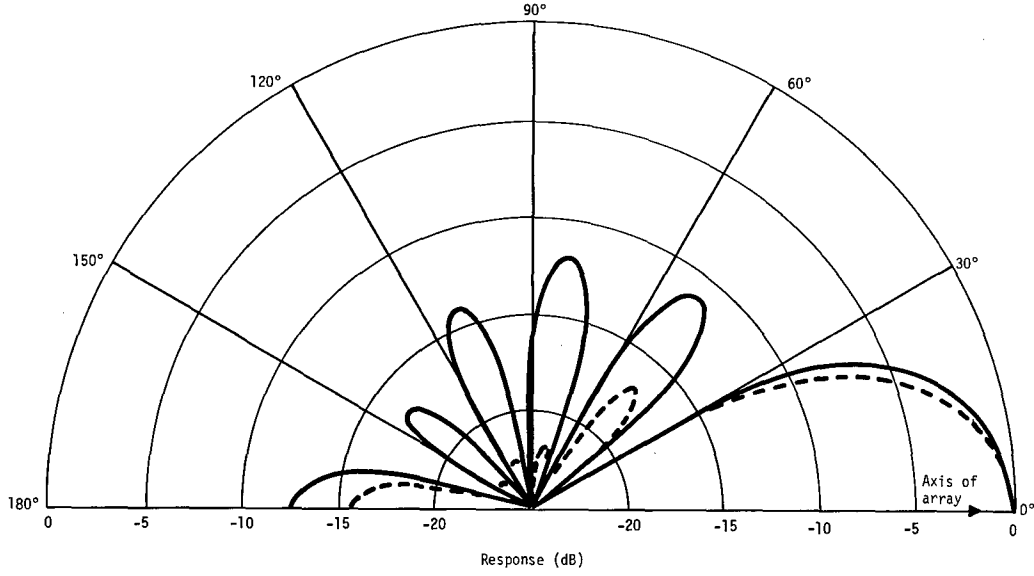
13

Fig. 9. Directional responses of six-element superdirective
array; maximum directivity index, end fire; three-dimensional
response is the figure of revolution about the axis of the
array; solid line, $\pi d/\lambda = 1$; dashed line, $\pi d/\lambda \ll 1$.

response normal to the axis of the array. Consider a superdirective
array of (n + 1) elements whose maximum directivity occurs at $\theta = \pi/2$.
The directivity index of such an array in which the element spacing
approaches zero is given by

$$D.I. = 10 \log_{10} D, \tag{36}$$

where

$$D = \frac{4 \left[F(\theta = \pi/2) \right]}{\int_0^\pi 2\pi \sin \theta \, F(\theta) \, d\theta}, \tag{37}$$

and

$$F(\theta) = \prod_{i=1}^{n} (\alpha_i + \cos \theta)^2$$

$$= (a_1 + a_2 \cos \theta + \cdots + a_n \cos^{n-1}\theta + \cos^n\theta)^2. \tag{38}$$

For n = 2 (three elements), D_2 becomes

$$D_2 = \frac{a_1^2}{a_1^2 + (1/3)(a_2^2 + 2a_1) + (1/5)}. \tag{39}$$

14

Taking the partial derivative with respect to a_2 and setting it equal to zero yields $a_2 = 0$. Taking the partial derivative with respect to a_1 and setting it equal to zero yields $a_1 = -3/5$. Substituting back into Eq. (39) yields $D_2 = 9/4$, which agrees with Pritchard's earlier results. The nulls of the resulting directional response are defined by

$$(-3/5) + \cos^2 \theta = 0,$$

$$\cos \theta = \pm\sqrt{3/5},$$

or

$$\tau_1 = \sqrt{3/5}(d/c); \qquad \tau_2 = -\sqrt{3/5}(d/c), \tag{40}$$

where d is the element spacing and c is the wavefront velocity. Similarly, for n = 4 (five elements),

$$D_4 = \frac{a_1{}^2}{a_1{}^2+(1/3)(a_2{}^2+2a_1a_3)+(1/5)(a_3{}^2+2a_2a_4+2a_1)+(1/7)(a_4{}^2+2a_3)+(1/9)}. \tag{41}$$

Taking the partial derivatives with respect to the a_i, setting them equal to zero, and solving the resulting set of equations yields

$$a_2 = a_4 = 0,$$

$$a_1 = 5/21, \qquad a_3 = -10/9,$$

$$D_4 = \left(\frac{3 \cdot 5}{2 \cdot 4}\right)^2 \tag{42}$$

$$\text{D.I.} = 5.46 \text{ dB.}$$

This, again, agrees with Pritchard's earlier results. The nulls in the directional response of the 5-element array are defined by

$$\cos \theta = \pm(1/3)\sqrt{5 \pm \sqrt{40/7}} \tag{43}$$

and the necessary delays by

$$\tau_1 = 0.90618(d/c) \qquad \tau_2 = -0.90618(d/c)$$

$$\tau_3 = 0.53847(d/c) \qquad \tau_4 = -0.53847(d/c) \tag{44}$$

Note that the nulls in both the 3-element and 5-element arrays are symmetrical about $\theta = \pi/2$ and that the necessary delays are such that positive and negative delays appear in pairs. This means that for single-frequency excitation, the phase shading in the different delay lines will cancel, leaving a purely real number for the shading coefficient as is illustrated in the vector representation for a 5-element array, Fig. 10.
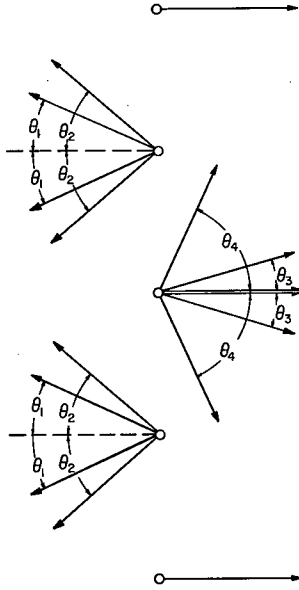
Fig. 10. Vector representation of Pritchard shading.

$$\theta_1 = \cos^{-1}\left[(2\pi d/\lambda)(0.53847)\right]$$
$$\theta_2 = \cos^{-1}\left[(2\pi d/\lambda)(0.90618)\right]$$
$$\theta_3 = \cos^{-1}\left[(2\pi d/\lambda)(0.36771)\right]$$
$$\theta_4 = \cos^{-1}\left[(2\pi d/\lambda)(1.44465)\right]$$

The weighting factors for a 3-element array are:

$$A_0 = 1,$$

$$A_1 = -2 \cos\left[(\omega d/c)\sqrt{3/5}\right] = -2 \cos\left[(2\pi d/\lambda)\sqrt{3/5}\right], \qquad (45)$$

$$A_2 = 1.$$

When $d \ll \lambda$, Eq. (45) can be approximated by

$$A_0 = 1,$$

$$A_1 = -2 + (3/5)(2\pi d/\lambda)^2, \qquad (46)$$

$$A_2 = 1.$$

For the 5-element array, the shading coefficients are:

$$A_0 = 1,$$

$$A_1 = -2 \cos\left[(\omega d/c)(0.90618)\right] - 2 \cos\left[(\omega d/c)(0.53847)\right],$$

$$A_2 = 2 + 2 \cos\left[(\omega d/c)(1.44465)\right] + 2 \cos\left[(\omega d/c)(0.36771)\right], \qquad (47)$$

$$A_3 = A_1,$$

$$A_4 = A_0 = 1.$$

Figure 8 is an illustration of Eq. (47), where the angles shown are based upon $d = \lambda/8$. It can be seen from the figure that if $d \to 0$, then θ_1, θ_2, θ_3, and θ_4 also approach zero, and, in the limit, the shading approaches that derivable from a binomial expansion (with alternating signs). When $d \ll \lambda$, Eq. (47) can be approximated by

16

$$A_0 = 1,$$

$$A_1 = -4 + (10/9)(\omega d/c)^2,$$

$$A_2 = 6 - (20/9)(\omega d/c)^2, \tag{48}$$

$$A_3 = -4 + (10/9)(\omega d/c)^2,$$

$$A_4 = 1.$$

Superdirectivity as described by Pritchard then can be thought of as being achieved by a perturbation of the binomial shading with alternating signs. In the limit $(d \to 0)$, the shading coefficients are binomial, but, without the perturbation (however small), the directivity function at $\theta = \pi/2$ is zero. This is important because of some misinterpretations of Pritchard's work. Urick [7], for example, states: "The properties of superdirectivity were pointed out by Pritchard. For example, the directivity index of an array of five elements one-eighth wavelength apart--and thus only one-half wavelength long--and having shading factors +1, -4, +6, -4, +1 was computed to be 5.6 dB ...." From Eq. (47), the correct shading factors would be

$$A_0 = 1,$$

$$A_1 = -2 \cos (\pi/4)(0.90618) - 2 \cos (\pi/4)(0.53847) = -3.338,$$

$$A_2 = 2 + 2 \cos (\pi/4)(1.44465) + 2 \cos (\pi/4)(0.36771) = 4.762, \tag{49}$$

$$A_3 = A_1 = -3.338,$$

$$A_4 = A_0 = 1.$$

Gradient Response of Superdirective Array

Equation (25) describes the response of an $(n + 1)$-element array of the type proposed in this report, where $|\tau_i| \leq \tau_0$ and $\tau_0 \to 0$. This equation is rewritten below:

$$m(t) = S\left\{ \prod_{i=1}^{n} (\tau_i + \tau_0 \cos \theta) \right\} \frac{\partial^n p(t)}{\partial t^n}. \tag{50}$$

Note that $m(t)$ is related to $\partial^n p(t)/\partial t^n$ rather than to $p(t)$. Consider a plane-wave field described by $p(t - x/c)$, where x is the direction of propagation. The n-th order gradient of this field evaluated at $x = 0$ is given by

$$\left. \frac{\partial^n p(t - x/c)}{\partial x^n} \right|_{x=0} = (-1/c)^n \frac{\partial^n p(t)}{\partial t^n}. \tag{51}$$

17

It can be said, then, that the array responds to the n-th order gradient of the field rather than to the field itself for the conditions assumed. If τ_0 does not approach zero, Eq. (12) gives a description of the response. That equation is rewritten below:

$$m(t) = f(t) - \sum_{i}^{n} f(t - b_i) + \sum_{i,j}^{n} f(t - b_i - b_j)$$

$$- \sum_{i,j,k}^{n} f(t - b_i - b_j - b_k) + \cdots \qquad (52)$$

$$\cdots (-1)^n f(t - b_1 - b_2 - \cdots - b_n),$$

where $b_i = \tau_i + \tau_0 \cos \theta$. If each term on the right-hand side of Eq. (52) is expanded in a Taylor series around $f(t)$, the resulting coefficients for $f(t)$, $\partial f(t)/\partial t$, $\cdots \partial^{n-1} f(t)/\partial t^{n-1}$ vanish. A general statement, then, that the arrays considered in this report are strictly higher order field gradient sensors is correct.

Practical Aspects of Superdirective Arrays

In the author's opinion, the Navy's acoustical community has failed to capitalize on the unique characteristics of superdirective arrays. One possible reason for this might be a misunderstanding of the price that one must pay for a superdirective array and the problems that are associated with its implementation. Certainly, as is true with any gradient sensor, there is a problem in achieving the desired sensitivity, but it is the author's opinion that this has been magnified out of proper proportion. In the case of the 6-element end-fire array, it was shown that the sensitivity is three times that of an individual element for an element spacing of $d = \lambda/\pi$.

The most difficult problem associated with the arrays proposed here probably is the matching of the sensitivities of the individual elements. It is difficult to assess the magnitude of this problem without actually constructing such arrays, but it is felt that arrays with more than five or six elements probably are impractical.

Another problem is the provision of the proper delays. It is believed that this problem can be overcome by a digital implementation. Such implementation for a 5-element array is developed in Appendix A, more for illustrative purposes than as a specific proposed implementation. Although emphasis in preceding sections has been placed on maximizing the directivity index of the receiving array, the real advantage of the super-directive arrays probably is the ability to control individually the nulls in the directional response. This is true because of the general nonisotropic properties of the interfering noise in underwater acoustical systems. More often than not, the greatest part of the interference

arises from targets of secondary interest. Such nonisotropic noise could
result from self noise of the using platform, other Navy vessels acting
in consort, or wild traffic of little interest. It is the author's
opinion that arrays shaded according to the methods proposed in this
report offer considerable potential for discriminating against such non-
isotropic noise.

To illustrate the directivity that can be achieved with arbitrary
placement of nulls in the directional response, Figs. 11-14 show plots of
5-element arrays (four nulls) with various arbitrary values of α_i. Empha-
sis has been put upon placing nulls at arbitrary points between $\theta = 65°$
and $\theta = 180°$, with acceptable side-lobe response and maximum response at
$\theta = 0°$. The most obvious Navy application of such an array would be that
of a towed array operating in the low-frequency range with emphasis upon
performance in the stern sector. The array would be capable of discrimi-
nating effectively against the noise of the towing platform and Navy ves-
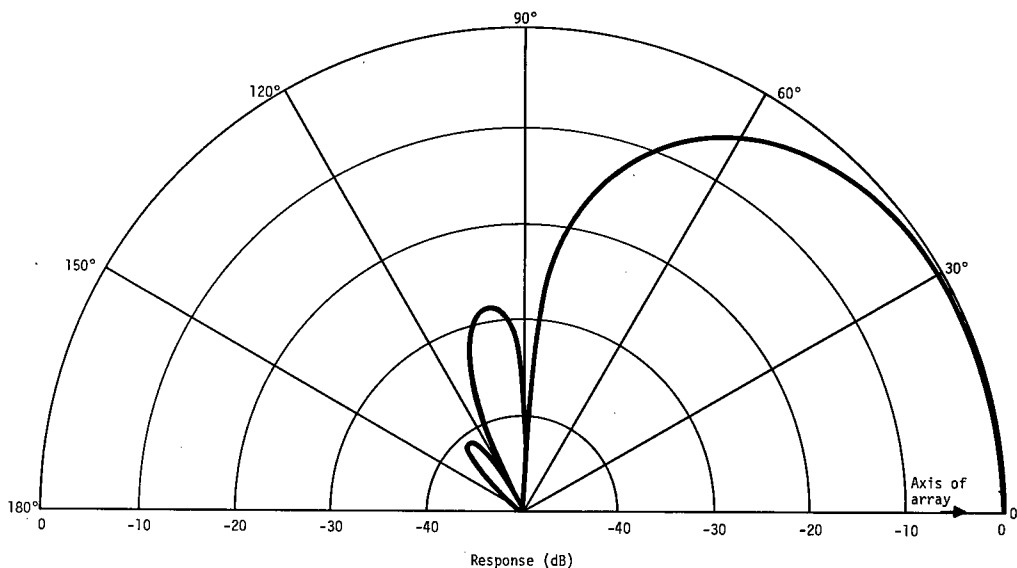sels acting in consort.

Fig. 11. Directional response of five-element superdirective
array with arbitrary nulls; three-dimensional response is the
figure of revolution about the axis of the array;

$$P_m(f) = 256P(f) \prod_{i=1}^{4} \sin^2[(\pi d/\lambda)(\alpha_i + \cos \theta)]; \quad \pi d/\lambda = 1;$$

$\alpha_1 = 1; \alpha_2 = 0.86603; \alpha_3 = 0.5; \alpha_4 = 0; [P_m(f,0)]/P(f) = 136.5.$

Another application might be the system concept illustrated in
Fig. 15, where the outputs of two end-fire superdirective arrays are
physically separated and their outputs correlated. The steerable nulls
could be identical in each array and be used to discriminate against
undesired targets. There is also no reason why superdirective arrays
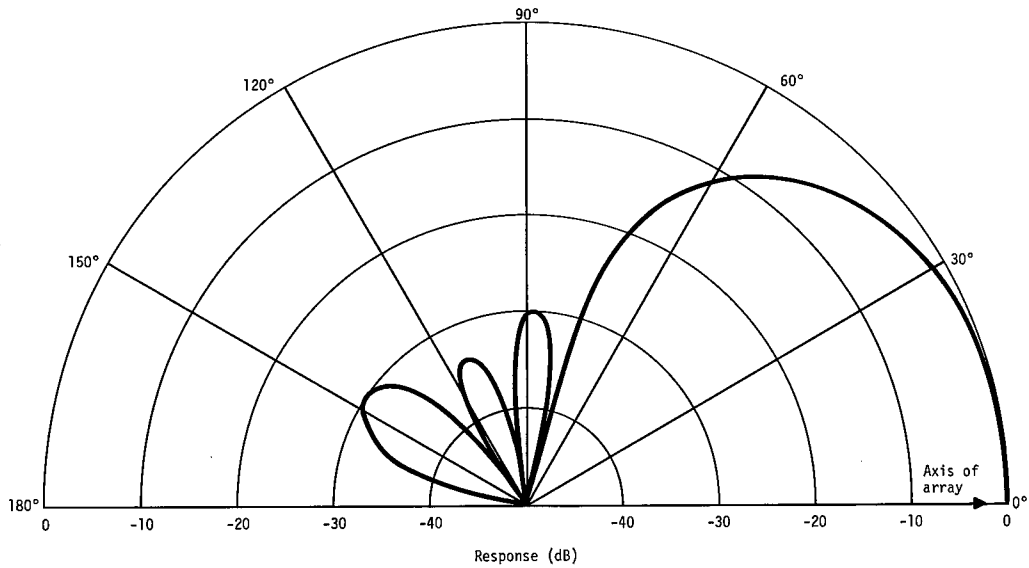could not be used as basic elements in conventional arrays.

Fig. 12. Directional response of five-element superdirective array with arbitrary nulls; three-dimensional response is the figure of revolution about the axis of the array;

$$P_m(f) = 256P(f) \prod_{i=1}^{4} \sin^2[(\pi d/\lambda)(\alpha_i + \cos \theta)]; \quad \pi d/\lambda = 1;$$

$\alpha_1 = 1; \; \alpha_2 = 0.6; \; \alpha_3 = 0.2; \; \alpha_4 = -0.2; \; [P_m(f,0)]/P(f) = 94.54.$

Fig. 13. Directional response of five-element superdirective array with arbitrary nulls; three-dimensional response is the figure of revolution about the axis of the array;

$$P_m(f) = 256P(f) \prod_{i=1}^{4} \sin^2[(\pi d/\lambda)(\alpha_i + \cos \theta)]; \quad \pi d/\lambda = 1;$$

$\alpha_1 = 1; \; \alpha_2 = 0.7; \; \alpha_3 = 0.2; \; \alpha_4 = -0.3; \; [P_m(f,0)]/P(f) = 75.04.$
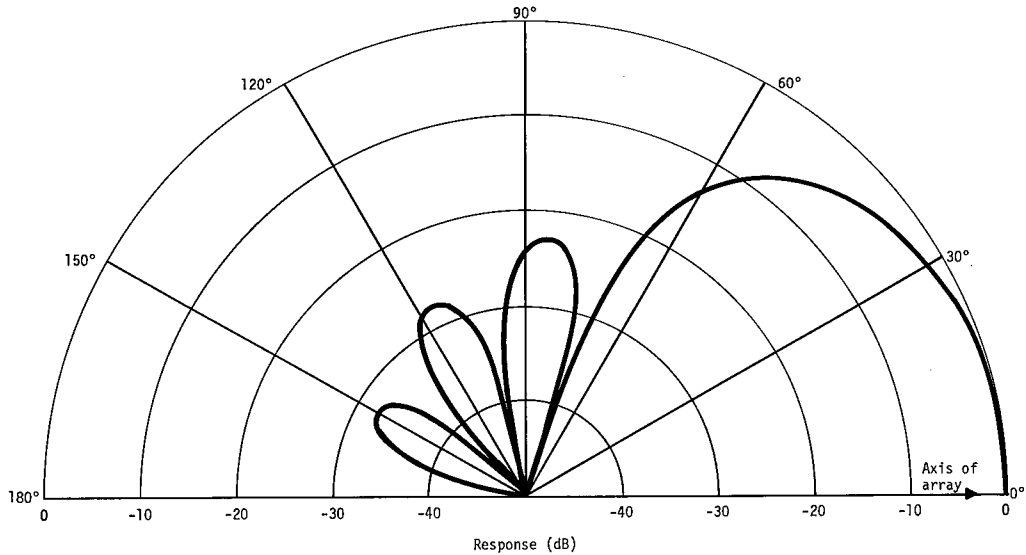
20
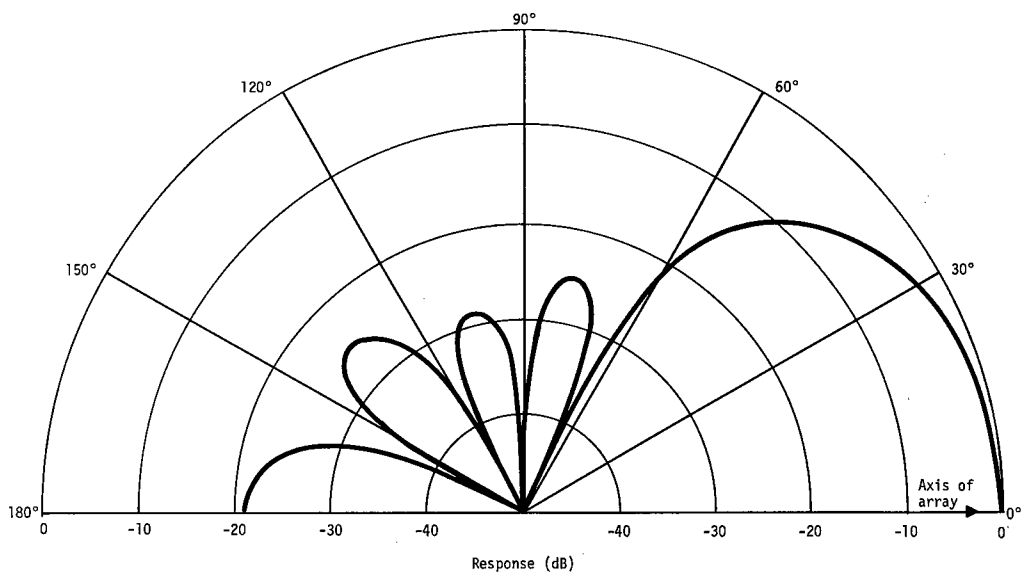
Fig. 14. Directional response of five-element superdirective array with arbitrary nulls; three-dimensional response is the figure of revolution about the axis of the array;

$$P_m(f) = 256P(f) \prod_{i=1}^{4} \sin^2[(\pi d/\lambda)(\alpha_i + \cos\theta)]; \quad \pi d/\lambda = 1;$$

$\alpha_1 = 0.9; \quad \alpha_2 = 0.467; \quad \alpha_3 = 0.033; \quad \alpha_4 = -0.4;$
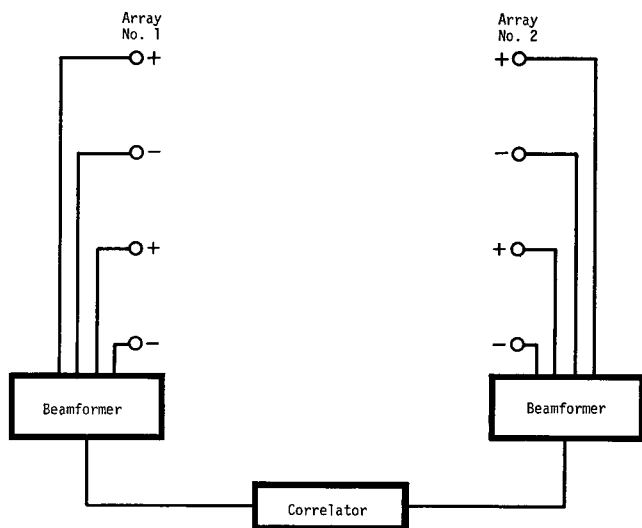
$[P_m(f,0)]/P(f) = 53.33.$

Fig. 15. Correlation system using super-directive arrays.

References

1. C. L. Dolph, "A Current Distribution for Broadside Arrays which Optimizes the Relation between Beam Width and Side Lobe Level," Proc. IRE 34, 335-348 (1946).

2. H. J. Riblet, discussion of Ref. 1, Proc. IRE 35, 489-492 (1947).

3. R. L. Pritchard, "Optimum Directivity Patterns for Linear Arrays," Acoustics Research Laboratory, Harvard University, Tech. Memo. No. 7, 12 May 1950.

4. R. L. Pritchard, "Directivity of Acoustic Linear Point Arrays," Acoustics Research Laboratory, Harvard University, Tech. Memo. No. 21, 15 Jan 1951.

5. R. L. Pritchard, "Optimum Directivity Patterns for Linear Point Arrays," J. Acoust. Soc. Amer. 25, 879-891 (1953).

6. R. L. Pritchard, "Maximum Directivity Index of a Linear Point Array," J. Acoust. Soc. Amer. 26, 1034-1039 (1954).

7. R. J. Urick, *Principles of Underwater Sound for Engineers* (McGraw-Hill Book Co., Inc., New York, 1967).

Appendix A

Digital Implementation of a Superdirective Array with Steerable Nulls

A system concept will be presented for digital processing of a five-element linear array with an element spacing equal to λ/π at the highest frequency to be processed. The aim of the system will be to derive four steerable nulls from the combination of the five elements. From Fig. 1 of the report, it is seen that the desired combination is given by

$$m(t) = H_0(t) - H_1(t - \tau_1) - H_1(t - \tau_2) - H_1(t - \tau_3) - H_1(t - \tau_4)$$

$$+ H_2(t - \tau_1 - \tau_2) + H_2(t - \tau_1 - \tau_3) + H_2(t - \tau_1 - \tau_4) + H_2(t - \tau_2 - \tau_3)$$

$$+ H_2(t - \tau_2 - \tau_4) + H_2(t - \tau_3 - \tau_4) - H_3(t - \tau_2 - \tau_3) \qquad (A1)$$

$$- H_3(t - \tau_1 - \tau_2 - \tau_4) - H_3(t - \tau_1 - \tau_3 - \tau_4) - H_3(t - \tau_2 - \tau_3 - \tau_4)$$

$$+ H_4(t - \tau_1 - \tau_2 - \tau_3 - \tau_4).$$

A digital sampled value of $m(t)$ can be obtained by digitally sampling the individual hydrophones at appropriate times and combining the results in an accumulator.

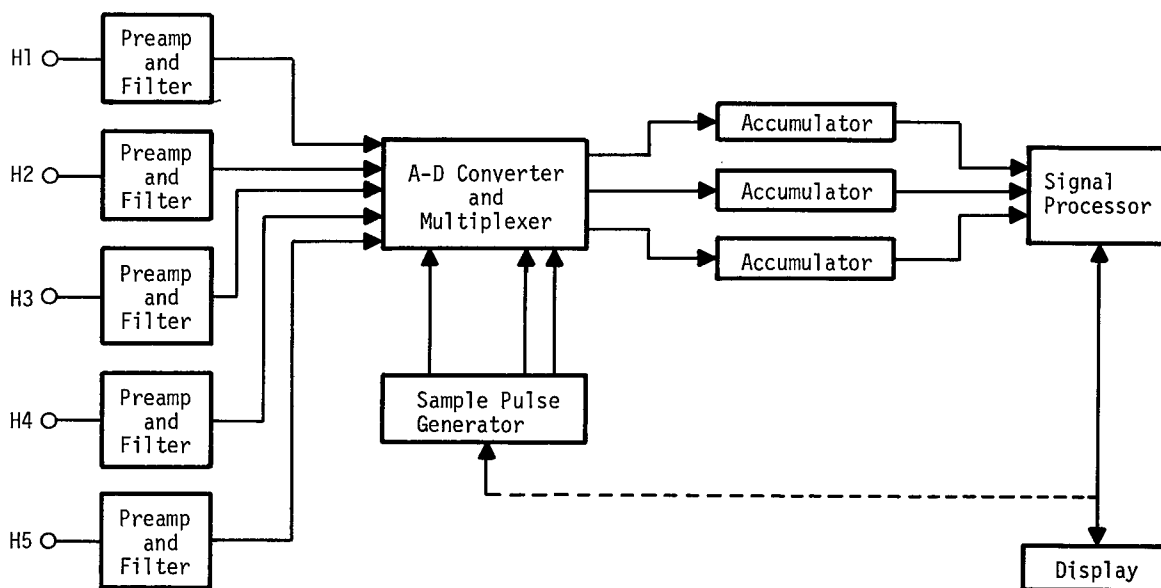Fig. A1. Steerable null system for five-element superdirective array.

Figure A1 illustrates, in block diagram form, the basic system concepts. The output of each hydrophone is passed through a preamplifier and filter where the signals are constrained to frequencies below the highest frequency to be processed and are conditioned in an appropriate form. It should be remembered that the ultimate response is primarily

23

to the fourth-order gradient of the signal and thus will result in considerably more emphasis on the higher frequencies processed. For this reason, it probably is desirable that the signal conditioning have the capability of providing up to 24 dB per octave boost for the low end of the spectrum. The preamplifiers and the signal conditioning for each channel will have to be very carefully matched both in amplitude and phase response. This is probably the most critical part of the design and can be adequately assessed only by construction of a prototype model. The outputs of these preamplifiers and filters are fed into a multichannel A-D converter and multiplexer. Sample time and channel information are provided to the converter and multiplexer by the Sample Pulse Generator. This generator instructs the multiplexer which hydrophone to sample and when to sample it and whether the results should be added to or substracted from the appropriate accumulator.

A block diagram of a Sample Pulse Generator is shown in Fig. A2. Four clock lines (C1, C2, C3, and C4) are generated by the 1-MHz clock and the three 0.2-μsec delays. These clock pulses can be operated on independently and the results combined. The master counter is a scale counter that allows the 1-MHz clock to be counted down and a "set" pulse derived at the appropriate Nyquist rate. Flip flop FF1 keeps the "and" gate that controls clock pulse C1 normally closed. When the "set" pulse is applied to the set input of FF1, the "and" gate allows the clock pulses from C1 to be applied to the "A" line and to the resettable scale counter SC1. When the preset count in SC1 is reached, a pulse is generated to reset FF1 and close the associated "and" gate. If the scale count of SC1 is set on the value A, there would then be A pulses on the "A" line for each sample period. Similarly, B and C pulses will appear on the "B" and "C" lines if SC2 and SC3 are set respectively at "B" and "C" counts. The C4 clock is controlled by flip flop FF4. The $\overline{D}$ line is fed by the C4 line through an "and" gate that is normally open. When the "set" pulse is applied to FF4, that gate is closed by FF4 for the number of counts that is preset into SC4. This is to allow a delay τ_4 of opposite sign to τ_1, τ_2, and τ_3. The scale counters C_{01} through C_{41} are used to generate the sample pulses. All of these counters are set to give a sample pulse after a fixed number N counts. Each counter is controlled internally to set itself to zero at the "set" pulse and to start counting. After a given counter has generated its sampling pulse, counts to it are inhibited until the next "set" pulse is received. Pulses to these counters come from the "or" gates shown, where the inputs to the "or" gates are from the appropriate gated clock. For example, the sample pulse from C_{01} will be generated at that time T_{01} after the set pulse given by

$$A + B + C + T_{01}/p - D = N,$$

or

$$T_{01} = p(N - A - B - C + D), \tag{A2}$$

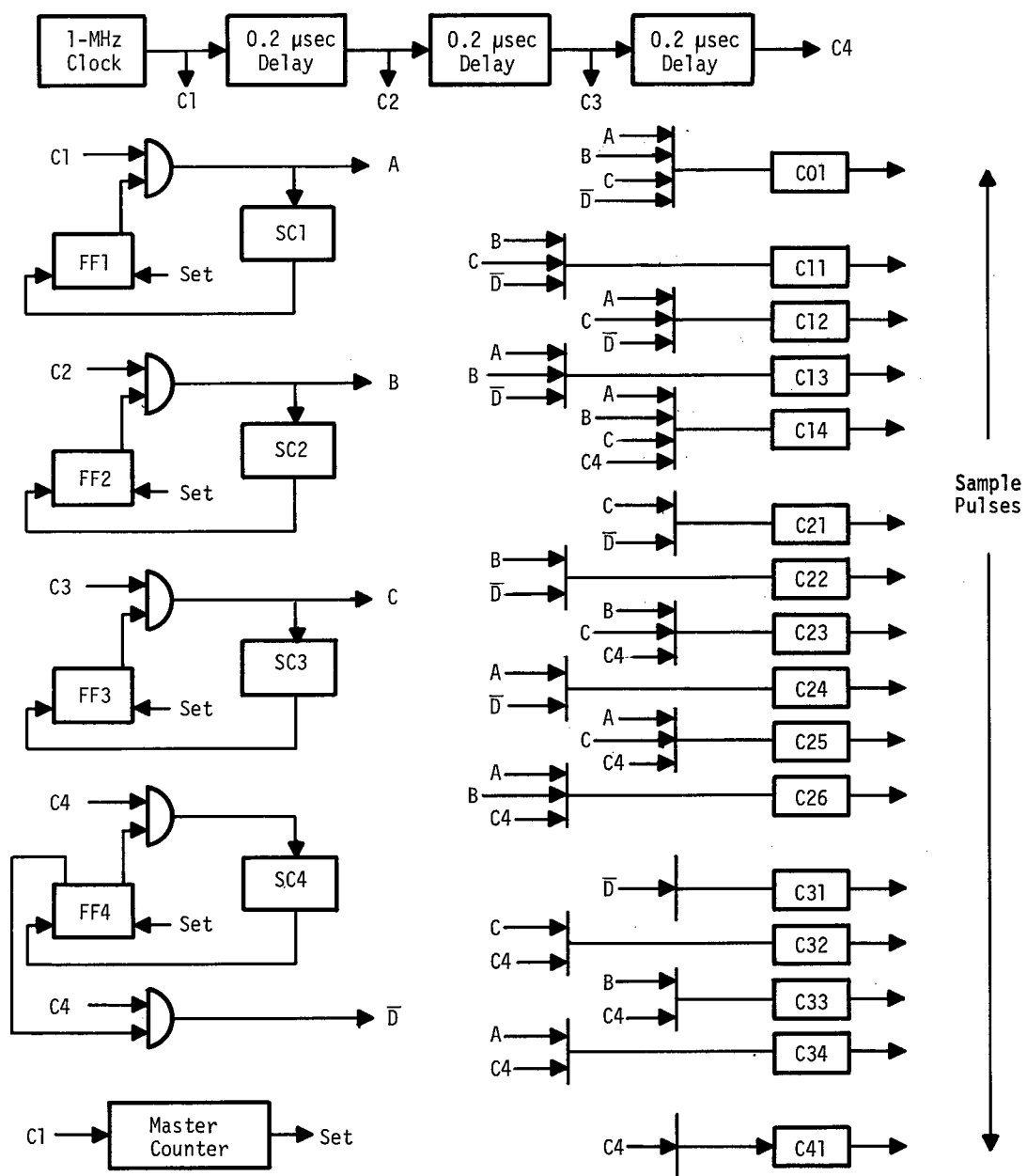where p is the basic clock period (1 μsec in this instance). The T for all of the sample pulses are shown below:

Fig. A2. Sample pulse generator.

$$T_{01} = p(N - A - B - C + D) \qquad T_{11} = p(N - B - C + D)$$

$$T_{12} = p(N - A - C + D) \qquad T_{13} = p(N - A - B + D)$$

$$T_{14} = p(N - A - B - C) \qquad T_{21} = p(N - C + D)$$

$$T_{22} = p(N - B + D) \qquad T_{23} = p(N - B - C)$$

$$T_{24} = p(N - A + D) \qquad T_{25} = p(N - A - C) \qquad \text{(A3)}$$

$$T_{26} = p(N - A - B) \qquad T_{31} = p(N + D)$$

$$T_{32} = p(N - C) \qquad T_{33} = p(N - B)$$

$$T_{34} = p(N - A) \qquad T_{41} = pN$$

If T_{41} is used to sample H_0, T_{3i} to sample H_1, T_{2i} to sample H_2, T_{1i} to sample H_3, and T_{01} to sample H_4, the delays of Eq. (A1) are satisfied, where

$$\tau_1 = Ap, \qquad \tau_2 = Bp, \qquad \tau_3 = Cp, \qquad \tau_4 = -Dp. \qquad \text{(A4)}$$

Since the τ_i control the positions of the nulls, the settings of scale counters SC1 through SC4 control these nulls. A dotted line is shown in Fig. A1 connecting the Signal Processor and the Sample Pulse Generator. The purpose of this is to indicate the possibility of having the resettable scale counters (and thus the nulls) under the control of the signal processor.

One consideration that has to be taken care of in the design is the possibility that the sample pulses for a given sample of m(t) will be distributed over a time interval larger than the Nyquist interval. One method to handle this would be to have those counters (probably C31, C32, C34, C41) that would be required to count for more than one sample at a given time appear in pairs.

As was stated earlier, the concept presented is not intended as a proposal, but to indicate the comparative ease with which the null processing can be implemented. The Sample Pulse Generator could be fabricated in an extremely small volume with an extremely low power drain, if integrated circuit logic were used. All other blocks of Fig. A1 are either commercially available or are standard items. Digital implementation was chosen for the illustration because it is believed that digital methods offer the greatest opportunity to preserve the accuracy necessary for implementation of null receivers based upon the principles stated in this report.

DOCUMENT CONTROL DATA - R & D

(Security classification of title, body of abstract and indexing annotation must be entered when the overall report is classified)

1. ORIGINATING ACTIVITY *(Corporate author)*	2a. REPORT SECURITY CLASSIFICATION
Naval Research Laboratory Underwater Sound Reference Division P. O. Box 8337, Orlando, Florida 32806	Unclassified
	2b. GROUP

3. REPORT TITLE

A NEW APPROACH TO SUPERDIRECTIVE ARRAYS

4. DESCRIPTIVE NOTES *(Type of report and inclusive dates)*
An interim report

5. AUTHOR(S) *(First name, middle initial, last name)*

A. Z. Robinson

6. REPORT DATE	7a. TOTAL NO. OF PAGES	7b. NO. OF REFS
5 January 1971	iii + 26	7

8a. CONTRACT OR GRANT NO. NRL Problem S02-30 b. PROJECT NO. RF 05-111-401--4471 c. d.	9a. ORIGINATOR'S REPORT NUMBER(S) NRL Report 7241 9b. OTHER REPORT NO(S) *(Any other numbers that may be assigned this report)*

10. DISTRIBUTION STATEMENT

This document has been approved for public release and sale; its distribution is unlimited.

11. SUPPLEMENTARY NOTES	12. SPONSORING MILITARY ACTIVITY Department of the Navy (Office of Naval Research) Arlington, Va. 22217

13. ABSTRACT

The concept of defined nulls in the directional response of arrays and the introduction of electrical delays to achieve the desired placement of the nulls provide a new approach to acoustical superdirective arrays. The shading that results is a variant of binomial shading in that the number of times a given element contributes to the array output is determined by the appropriate binomial coefficient, but the signal from the element undergoes a possibly different electrical delay each time the element contributes. For an end-fire condition, the maximum array gain (assuming isotropic noise) is equal to the square of the number of elements in the array. The methods used yield results for three- and five-element broadside arrays that are equivalent to those obtained earlier by R. L. Pritchard. The type of array described responds to a higher order gradient of the pressure field rather than to the pressure field itself. A digital method for implementation of such an array is presented.

14. KEY WORDS	LINK A		LINK B		LINK C	
	ROLE	WT	ROLE	WT	ROLE	WT
Transducer arrays						
Superdirectivity						
Signal processing						